Journal of Power Sources 609 (2024) 234704

Contents lists available at ScienceDirect

Journal of Power Sources

journal homepage: www.elsevier.com/locate/jpowsour

3D printing of reversible solid oxide cell stacks for efficient hydrogen production and power generation

A.M. Martos [a], S. Márquez [a], R.S. Pavlov [a], W. Zambelli [a], S. Anelli [a,b], M. Nuñez [a], L. Bernadet [a], J.J. Brey [c], M. Torrell [a], A. Tarancón [a,d,*]

[a] IREC, Catalonia Institute for Energy Research, Jardins de les Dones de Negre 1, 2nd Floor, Sant Adrià del Besós, 08930, Barcelona, Spain
[b] Polytechnic of Turin, Department of Applied Science and Technology DISAT, Corso Duca Abruzzi 24, I-10129, Turin, Italy
[c] Engineering Department, Universidad Loyola Andalucía, Avenida de las Universidades s/n, Dos Hermanas, 41700, Sevilla, Spain
[d] ICREA, Passeig Lluís Companys 23, 08010, Barcelona, Spain

HIGHLIGHTS

- 3D printed scalable large-area electrolyte-supported SOCs are fabricated.
- Ultra-compact stack is developed based on 3D-cells and flat thin interconnects.
- Innovative stacks deliver three times the power density of their planar counterparts.
- 300-W reversible-SOC stacks based on 3D printed cells are tested.

ARTICLE INFO

Keywords:
3D printing
Solid oxide cell
Electrolysis
Electrolyte supported cell

ABSTRACT

Renewable hydrogen offers a promising pathway to address the challenge of large-scale chemical energy storage in the transition to a decarbonized future. The most efficient devices to convert renewable electricity into hydrogen, and vice versa, are reversible solid oxide cells (SOC-s). Despite recent advances in materials performance and durability, conventional ceramic manufacturing technologies strongly limit the huge potential of SOC-s, imposing severe geometrical restrictions that penalize the overall system efficiency. Here we capture the benefits of using previously unexplored complex-shapes by scaling 3D-printed reversible solid oxide cells with improved mechanical properties, higher performance, and embedded functionality. Stacks made of 45 cm^2-3D-printed electrolyte-supported solid oxide cells combined with ultrathin flat metallic interconnects were successfully fabricated and operated in fuel cell (SOFC) and electrolysis (SOEC) modes delivering up to 85 L/h of hydrogen production while presenting less than 5 % degradation after more than 500 h of operation. The advances presented here demonstrate the viability of upscaling the process of solid-oxide-cell 3D printing and brings advantageous stack designs aimed for a cost-competitive and customizable hydrogen technologies deployment. In particular, the enhancement by design achieved here provides innovative SOC stacks with volumetric and gravimetric power densities that are three and four times higher, respectively, than their planar counterparts using the same set of materials.

1. Introduction

Green hydrogen is the best candidate for an efficient long-term chemical energy storage of the intermittent power generated by renewable sources presenting a smart solution for decarbonizing energy-intensive sectors such as the heavy transport and chemical industries [1]. The use of renewable electricity to produce green hydrogen is often called Power-to-Gas (PtG) or, more generally, Power-to-X (PtX) when hydrogen is catalytically converted downstream into different fuels and other valuable products [1]. Among the different types of electrolysis systems, those based on high temperature Solid Oxide Electrolysis Cells (SOECs) are, by far, the most efficient ones with lower specific electric energy (<40 kWh/kg of H_2) than competing technologies (>50 kWh/kg for alkaline and > 55 kWh/kg for polymeric) [2,3]. Moreover, Solid

* Corresponding author. IREC, Catalonia Institute for Energy Research, Jardins de les Dones de Negre 1, 2nd Floor, Sant Adrià del Besós, 08930, Barcelona, Spain.
E-mail address: atarancon@irec.cat (A. Tarancón).

https://doi.org/10.1016/j.jpowsour.2024.234704
Received 15 March 2024; Received in revised form 3 May 2024; Accepted 8 May 2024
Available online 14 May 2024

Oxide Cells (SOCs) can efficiently operate in both electrolysis and fuel cell modes giving rise to reversible Solid Oxide Cells (rSOCs) that extend the PtG concept to roundtrip Power-to-Power (PtP) conversion schemes [4,5]. Impressive PtP round-trip efficiencies > 70 % have been simulated for rSOC systems, anticipating its relevance for seasonal storage applications with size constraints or where battery capacity is insufficient [6]. On the other hand, a system based on a commercial r-SOC system demonstrates an efficiency of approximately 55 % [7].

SOC technologies have undergone tremendous development over the past two decades mainly due to significant advances in materials design [8,9], increasing the performance of the devices and, more significantly, their durability, which is currently in the order of tens of thousands of hours of operation [2,10]. Indeed, several companies have produced commercial products based on SOC technology to be applied as fuel cells or electrolysis systems. However, at stack level, the progress has been much more gradual, note that the current systems are still based on cell and interconnect designs that did not experience drastic changes from the ones proposed in the early 90s [11]. This is mostly due to the large limitations of conventional ceramic manufacturing techniques that mainly restrict the shape of SOC cells to planar- and tubular geometries [12,13]. Some of the most relevant and disruptive approaches at the cell and stack level have been the flat tubular cell architectures [14–16], integrated planar cells on porous substrates proposed by Rolls-Royce [17], or the advances of Siemens in using a characteristic design based on a multiple cell array concept on a metal plate [18]. Note that some modeling studies have also been done, aligned with the membrane corrugation approach [19] the 3D printing [20,21] among other proposed geometries and architectures [22,23]. Nowadays, new emerging fabrication technologies such as 3D printing allow the creation of complex-shape geometries (even for highly refractory ceramics) opening new possibilities for developing advanced designs in SOCs and other energy technologies. In this regard, 3D printing has recently been extensively employed in SOC cells for layer deposition of the main components such as electrolytes, functional electrodes, or catalysts but mainly on top of existing substrates that maintain similar architecture constrains [24]. Indeed, the fabrication of cells with complex geometries (i.e. presenting high aspect ratio) is still limited to very few studies based on stereolithography (SLA) and digital light printing (DLP) of electrolyte-supported SOCs [25–27]. Among the very few complex-shape cells fabricated by 3D printing previously published, we recently presented the potential of electrolyte corrugation strategies as a disruptive approach to increase the performance of ceramic cells by design. In our previous work, we were able to fabricate 3D printed SOC button cells with high-aspect ratio that demonstrated a great performance (-600 mA/cm^2 at 1.3 V) with a 60 % increase compared to their flat counterpart and an excellent mid-term durability [25]. Despite this interesting result, the present work confirms for the first time the suitability of functional ceramic 3D printing technology for the development, manufacturing and scaling of a next generation SOC device based on complex shaped cells not previously reported and presenting relevant enhancements to the SOC stacks by design.

The present work explores a novel ultra-compact SOC stack concept based on standard-size electrolyte-supported corrugated cells fabricated by 3D printing. These complex-shaped cells are endowed with functionalities traditionally reserved for metallic interconnects, such as gas distribution, and mechanical support, leading to a remarkable reduction of the size, and weight of the final stack. Due to the use of state-of-the-art materials, the enhancement is achieved purely by design, keeping all the advantages of a champion combination of materials with excellent performance and, more importantly, high stability.

2. Experimental methods

Cell fabrication. Electrolyte-supported 3YSZ cells were prepared employing an industrial SLA 3D printer (Ceramaker C-1000 from 3DCERAM SINTO, France) using a doctor blade approach. Computer-aided design (CAD) models of the corrugated cells were imported into an SLA 3D printer, which layered the model into 50 μm slices for further printing. 3YSZ slurries developed by the printer's supplier (3DCERAM SINTO, France) were used as a printable feedstock. These slurries consisted of an acrylate UV photocurable monomer, a photoinitiator, a plasticizer, a dispersant and 3YSZ ceramic powder. The 3YSZ slurry was deposited layer wise on a 300 × 300 mm^2 printing platform using a doctor blade system to achieve a homogenous film. Each layer was cured using a laser to form the desired patterns, followed by platform descent by 50 μm. The sequence was repeated until completing the green body electrolyte. After finishing the printing process, most of the slurry was drained from the green parts, and the uncured paste could be reused in later printings. Any trace of slurry, in the green printed electrolyte, was then removed by using a solvent (Ceracleaner®. 3DCERAM SINTO, France). The clean parts were submitted to a special thermal treatment in nitrogen atmosphere reaching a temperature of 800 °C for 2 h to ensure complete removal of the organic components without producing any cracks or other defects. Finally, the organic-free parts were sintered at 1450 °C for 2 h in air atmosphere, resulting in a dense 3YSZ part. For the preparation of the fuel (NiO-8YSZ) and oxygen (LSM-8YSZ) electrodes, commercial pastes (Fuel cell materials, USA) were manually applied on the electrolyte membranes. These layers were sintered in air in two steps at 1400 °C and 1200 °C for 2 h, respectively at a heating and cooling rate of 1 °C/min.

Sealing procedure and stack assembly. 200 μm-thick flat metallic sheets made of Crofer 22APU were cut and drilled for acting as interconnects in the stack. The interconnects were coated with manganese cobalt oxide (MCO) and sintered at 980 °C for 2 h. Alumina felts (AFS-100, Fuel cell materials, USA) impregnated with aqueous alumina suspension were employed. The alumina solution was impregnated on both faces to ensure a proper gas tightness. The components were aligned and mounted to form the complete stack according to the assembly diagram presented in Fig. 2a.

Characterization of the printable feedstock and the final devices: The slurries and electrolytes were characterized by using the following techniques: the rheological behavior of the commercial slurry was determined using a DHR-2 rheometer (TA Instruments, Waters, USA). For the measurements a circular geometry with parallel plates with 20 mm of diameter was used. The viscosity measure was repeated three times on different samples of paste and good reproducibility of the measurements and good accuracy of the measured viscosity values was observed (see Fig. S1 in Supplementary data). The initial viscosity was 16.4 Pa s and at shear rate of 200 s^{-1}, the viscosity was 3.7 Pa s, as it shown in Supplementary information S1. TGA experiments were carried out using a Mettler Toledo STAR^e TGA/DSC 1 System (Spain) under nitrogen, ranging from 25 to 800 °C at a heating rate of 25 °C/min. DSC measurements were performed under nitrogen with a Mettler Toledo DSC 3+ STAR^e System (Spain). The sample was heated from 25 to 600 °C at a heating rate of 25 °C/min, maintaining the temperature for 120 min at the end, followed by cooling at 50 °C/min. The sample was then reheated under the same conditions. This thermal analysis was important to decide the optimal debinding temperatures (see Fig. S2 in Supplementary information). X-ray diffraction analysis was carried out using a Bruker D8 Advance Diffractometer (USA) with Cu Kα radiation ($\lambda = 1.5418$ Å) in the 2θ range 20–90° (Fig. S3 in Supplementary data). The cross-section and the painted electrodes were characterized using a ZEISS Auriga 60 Field Emission Scanning Electron Microscope (FESEM, Zeiss, Germany), equipped with an energy-dispersive X-ray spectrometer (Oxford X-Max, United Kingdom). Optical microscopy of the corrugated profile was performed using Dino-Lite Edge Digital Microscope (AnMo Electronics Corporation, Taiwan) (see Supplementary information S1).

Electrochemical performance tests. Stacks were evaluated in home-designed test benches. In particular, the substack was gradually heated to 900 °C at a rate of 1 °C/min under 0.5 L/min nitrogen flow on both the fuel and oxygen electrodes. Upon reaching 900 °C, the fuel electrode

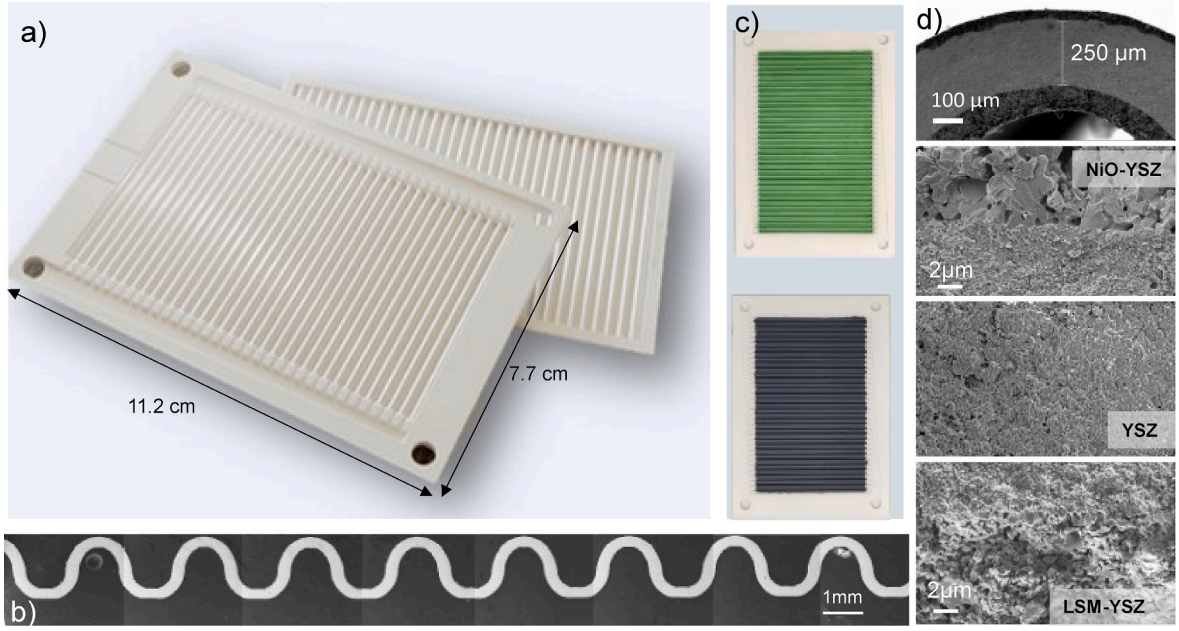

Fig. 1. 3D printed solid oxide cells: a) Photography of 3D-printed and sintered complex-shaped cells with embedded channels; b) Cross-section SEM image of the corrugated electrolyte membrane after sintering; c) Top-view images of both sides of the 3D printed electrolyte after functionalization with the fuel and oxygen electrodes (NiO-YSZ in green and LSM-YSZ in black, respectively); d) Cross-section SEM images of the complete cell, fuel electrode (top), electrolyte (central) and oxygen electrode (bottom). (For interpretation of the references to colour in this figure legend, the reader is referred to the Web version of this article.)

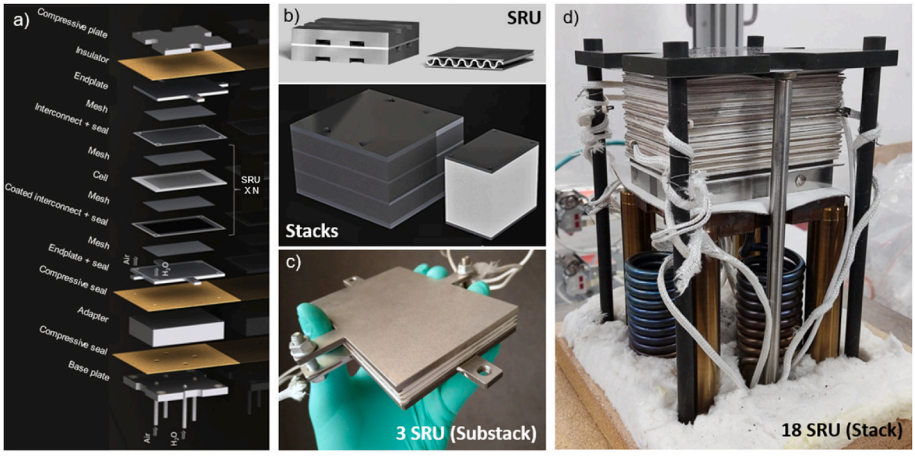

Fig. 2. Solid Oxide Cell stacks composed of 3D printed cells: a) A 3D rendering of the final stack assembly with all the components included, b) Comparison of single repeating units (SRU) and stacks based on conventional flat cells and our complex-shaped design, c) An operational substack containing three SRUs, d) Picture of a stack made of 18 SRUs.

(NiO-YSZ) was reduced by gradually increasing the quantity of H_2 in the gas mixture, eventually transitioning to pure H_2. After the reduction of the electrode was completed, the performance of the substack was characterized. Current/voltage (I–V) curves were obtained in SOFC mode, with the hydrogen and synthetic air flows of 2.65 L/min and 4.3 L/min, respectively. Subsequently, I–V curves were recorded in SOEC mode, where the fuel gas consisted of steam 5 L/min, H_2 0.5 L/min and N_2 0.5 L/min and the oxygen gas air of 2.65 L/min. A degradation test was performed under SOEC mode by applying −11 A at 900 °C. These tests provided crucial insights into the electrochemical performance of the substack under both fuel cell and electrolysis modes. In the case of stack, the flows used in SOEC mode were 7.5 L/min of steam, 1 L/min of hydrogen and 1 L/min of nitrogen on the fuel side and 8 L/min of synthetic air in the air side. The degradation of the stack was carried out applying −11 A at 900 °C. In both stacks measurements (3 and 18 cells), the steam concentration is 90 %, with the remaining 10 % consisting of hydrogen concentration. The characterization allowed for an understanding of the substack behavior at different operating conditions, including the effects of temperature, gas composition, and degradation over time.

3. Results

3.1. 3D printed solid oxide cells enhanced by design

Complex shape yttria-stabilized zirconia (YSZ) cells of different range of sizes were fabricated by using stereolithography (SLA). Careful optimization of the 3D printing and sintering processes made possible the scaling up of the dimensions (see details in section S2 of the Supplementary information). Fig. 1a shows examples of successfully manufactured defect-free YSZ parts with unique features, such as a thin corrugated electrolyte membrane, embedded gas distribution channels,

inlet and outlet gas holes and sealing frames. Such a corrugated electrolyte membrane straightforwardly by 60 % the active area of the counterpart flat cells, from 45 cm^2 (used as projected area for the calculations) to 72 cm^2 (enhanced active area) whilst ensures a proper fuel and air distribution along the cell (playing the role of the interconnect channels in conventional planar stacks) and enhances mechanical properties of the membrane for processing (cleaning, debinding, sintering). The geometry of the channels and manifolds was optimized by performing finite elements simulations targeting the reduction of the gas pressure drop while ensuring a uniform gas velocity across the cell (see section S3 in the Supplementary Information). Despite the high complexity, reduced thickness (250 μm) and large area of the corrugated electrolyte membranes presented in Fig. 1a, they are highly homogeneous, crack-free, and fully dense (Fig. 1b) suitable as SOC electrolytes. Moreover, according to thermomechanical simulations carried out in this work (S3 in the Supplementary Information), this innovative design notably improves the mechanical properties of the cells compared to their planar counterparts, thus overcoming one of the major issues arising for SOEC planar cells when operated under pressure.

In order to evaluate their performance, these complex-shaped electrolytes were functionalized with fuel and oxygen electrodes by the deposition of nickel-oxide (NiO-YSZ) and lanthanum-strontium-manganite (LSM-YSZ) composites, respectively, to produce complete SOC cells (Fig. 1c). The electrodes employed were selected among well-known state-of-the-art SOC materials, thus emphasizing the enhancement by design [28–30]. Despite this, comprehensive structural characterization of the fuel and oxygen electrodes was carried out (described in Supplementary Information S2). To verify the proper attachment between different layers and the density and homogeneity of the fabricated electrolyte, cross-section SEM images of the complete cell and the different parts of the cell were obtained (Fig. 1d). As can be seen, the electrolyte obtained is fully dense without cracks or delamination and has a small average grain size of around 400 nm (see Figs. S4 and S6 in the supplement information). At higher magnifications (included in the Supplementary data as Fig. S5) one can eventually observe the steps generated by the layer-by-layer nature of the printing process, experimentally confirming a nominal resolution of *ca.* 50 μm in all x-, y- and z-axes. Moreover, Fig. 1d reveals that the fuel and oxygen electrodes are highly porous and homogeneous (approximately 30 μm of thickness) exhibiting excellent adhesion with the electrolyte. Overall, it can be safely asserted that the complete cells produced in this work fully comply with the well-known features of high-quality cells manufactured by employing advanced ceramic processing.

3.2. 3D printed stacks with high volumetric and mass power density

More than 30 units of the complex-shaped cells were fabricated by 3D printing presenting a production yield of 85 %, which confirms the robustness of the manufacturing process. The high quality and reproducibility of the complete cells allowed us to produce and validate full stacks. Fig. 2a schematically shows a detail of a complete stack assembly with all the required components. The stack comprises metallic endplates sandwiching one or more single repeating units (SRUs) made of 200 μm-thick Crofer®22APU interconnects coated with manganese cobalt oxide (40 μm) and corrugated cells. For this work, two different stack assemblies were fabricated for electrochemical validation of the novel compact architecture as presented in the following section: a substack containing three SRUs (Fig. 2c) and a stack of 18 SRUs (Fig. 2d).

As illustrated in Fig. 2b, the use of our innovative cells with embedded functionalities strongly simplifies the conventional bulky and complex metallic interconnects converting them into plain thin flat sheets with holes [31,32]. Such a simplification of the interconnects represents an enormous advantage of our design in terms of cost and power density per unit mass since metallic parts represent more than 75 % of the total weight of the stack [33]. Moreover, the interconnect is much thinner and simpler than commonly used designs [34], so that the volume of the stack is reduced accordingly while making the manufacturing and assembly processes easier and cheaper [35]. According to simple calculations, our stack design increases up to three and four times the volume and mass specific power respectively, as compared to conventional planar cell. This gives rise to a new class of ultracompact and lightweight stacks (see Fig. 2b for a size comparison based on equally performing cells) [35–37]. The here presented improvement of the volumetric power density will allow SOCs to be used in a wider range of applications. Currently the typical commercial SOFCs are in the 0.1–1 kW/L range in volumetric power density [38,39], and it is predicted that improving the gravimetric power density of 1.0 kW/kg will allow the SOFC technology to enter to the aeronautic and aerospace applications [40]. In addition, the improved mechanical properties extracted from the model results of our corrugated cells (see Supplementary information S3) enable the safe use of compressive sealants even under high pressures. In this regard, despite the interest of employing compressive sealants, such a sealing strategy is generally discarded in commercial products due to mechanical issues. Among other advantages, compressive sealing strongly simplifies component substitution or selective dismantling of the stack, which is critical for recyclability and maintenance purposes.

3.3. Reversible performance in fuel cell and electrolysis mode

In order to validate our novel stack design, a substack module containing three SRUs based on corrugated cells and flat thin interconnects (sealed with compressive sealants) was measured in fuel cell and electrolysis mode. First, SOFC conditions were imposed by feeding the fuel electrode chamber with pure hydrogen and the oxygen electrode chamber with synthetic air. After reduction of the fuel electrode, an open circuit voltage (OCV) of 3.4 V, corresponding to 1.13 V per cell, was obtained at 900 °C. This OCV is in good agreement with the value expected from the Nernst's equation, which indicates an adequate gas tightness of the system that validates the overall quality of the electrochemical measurement. Polarization curves were subsequently measured in SOFC mode at the same temperature as shown in Fig. 3a (employing a continuous flow of 2.65 L/min H_2 for the fuel side and 4.3 L/min of synthetic air for the oxygen side). A total maximum power of 27 W (and −15 A of current) was obtained for the substack, which corresponds to a maximum power density of 200 mW/cm^2 (and −350 mA/cm^2 of current density). These power density values are consistent with previously reported data considering 3YSZ conductivity and thickness [26] confirming the feasibility of the 3D printed enabled design at stack level.

Complementary to SOFC measurements, the same substack was operated in SOEC mode at 900 °C employing steam mixed with hydrogen as a fuel (with a continuous flow of 5 L/min of steam, 0.5 L/min of hydrogen and 0.5 L/min of nitrogen) and synthetic air as an oxidant (with a continuous flow of 2.65 L/min). The OCV value was 2.26 V as it can be seen on the polarization curve represented in Fig. 3b. A total current of *ca.* −20 A was injected at 4.2 V (equivalent to ~85 W of power), which corresponds to a current density of −450 mA/cm^2 at 1.4 V per cell. The values obtained are again comparable to the ones reported in the literature for standard electrolyte-supported cells [41].

Overall, the results obtained in both SOEC and SOFC modes demonstrated a good performance of the substack. Complementary to performance measurements, mid-term stability tests were carried out in SOEC mode for hydrogen production. Galvanostatic conditions were imposed by applying −11 A (corresponding to 3.3 V, i.e. 1.1 V per cell) in SOEC mode. Fig. 3c shows the voltage evolution of the stack over 500 h of stable operation under constant current. The initial conditioning of the stack is considered for the first 250 h by convention [25]. The subsequent 250 h of operation were employed to formally evaluate the degradation. Considering this period, one can estimate the degradation rate of the substack to be slightly below 5 % per 1000 h (eventually

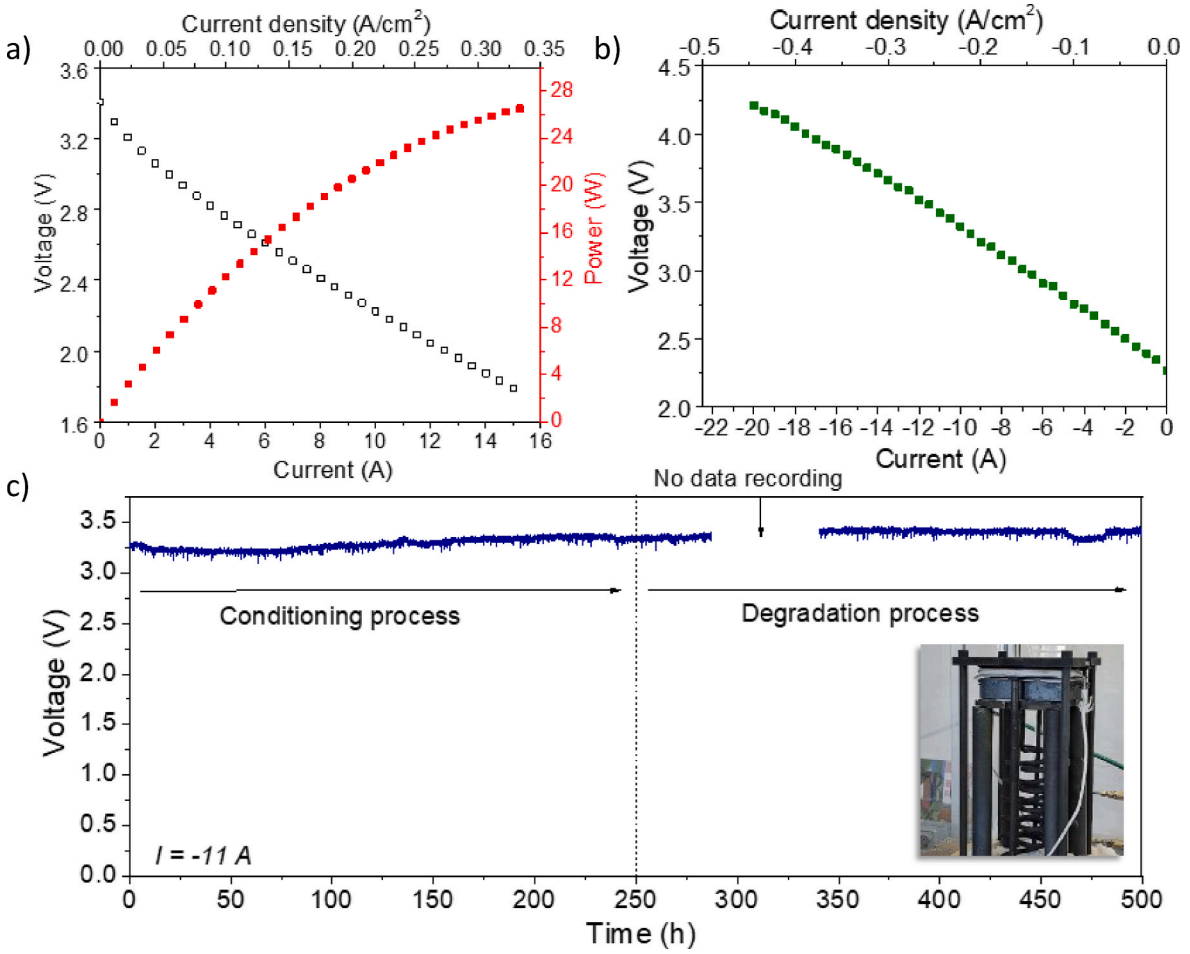

Fig. 3. Electrochemical characterization of stacks based on 3D printed SOC cells at 900 °C. a) I–V and power curves of a substack of 3 SRUs measured in SOFC mode; b) I–V curve of a substack of 3 SRUs measured in SOEC mode, c) Mid-term galvanostatic test of a stack of 3 SRUs (see insert) carried out in SOEC mode during 500 h at a fixed current of I = –11 A (slight voltage fluctuations during the test were caused by a certain instability in the steam generation while data recording was not possible in the range between 300 and 350 h.

improving during the last 100 h), which is considered a remarkable result considering that the presented work has been focused on the cell development and no on the optimization of the rest of the stack components. In this regard, the obtained result of stability on SOEC operation mode is considered compared to reported commercial SOC cells and stacks [2,25,42–45], confirming the stability of the novel stack architecture during operation in the mid-term regime.

Finally, 18 SRUs were assembled in a single stack and were tested in

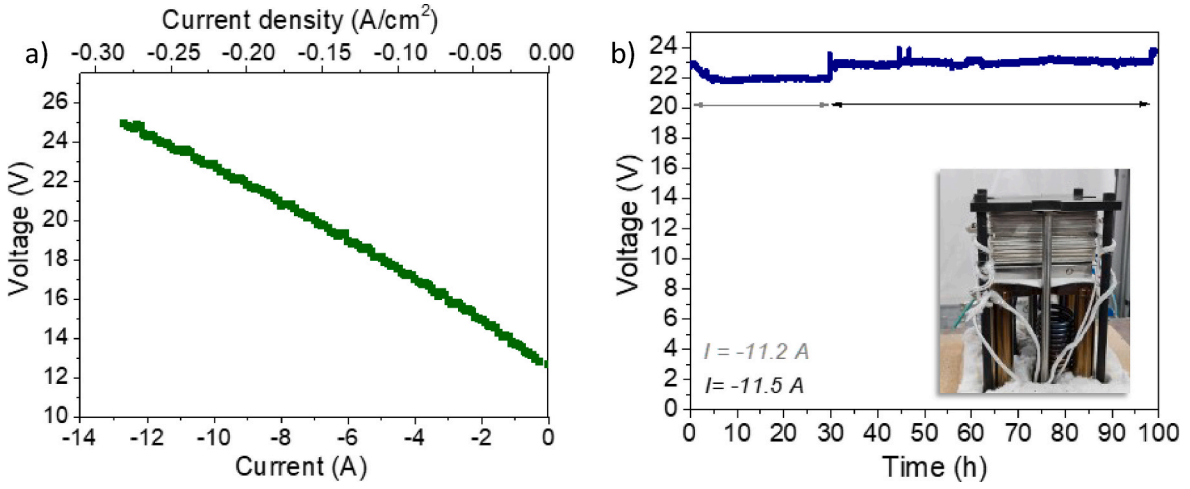

Fig. 4. Electrochemical characterization of stacks based on 3D printed SOC cells at 900 °C. a) I–V curve of a stack of 18 SRUs measured in SOEC mode; b) Short-term galvanostatic test of a stack of 18 SRUs (see inset) carried out in SOEC mode during 100 h at a fixed current of I ~ –11 A (two different regions are observed for readjustment of the current from 11.2 A to 11.5 A).

SOEC mode to definitely prove the suitability of the new architecture at stack level and the feasibility of the complete stacking procedure (Fig. 2d). The corresponding I–V curve at 900 °C is presented in Fig. 4a (under continuous flow of 7.5 L/min of steam, 1 L/min of hydrogen and 1 L/min of nitrogen in the fuel side and 8 L/min of synthetic air in the air side). According to these results, OCV values of 12.5 V were obtained together with a maximum injected current to *ca.* −13 A at 25 V (equivalent to 330 W of power), which corresponds to a current density of −290 mA/cm^2 at 1.4 V per cell. Although these values are lower than the ones achieved for the test of the substack, likely due to potential mismatches between the current collector meshes and the electrode leading to contact losses, they are still in the range of relevant current densities for commercial applications confirming the suitability of the new geometry for complete SOEC stacks. As a final test, the voltage evolution over 100 h of operation of the whole stack in SOEC mode was carried out at a fixed current density of *ca.* −11 A (corresponding to 22.5 V, i.e. 1.25 V per cell). Results are shown in Fig. 4b showing excellent behavior with no relevant degradation over the whole duration of the experiment.

Overall, the performance and operational stability test shown in this section proved the excellent performance and durability of the proposed novel concept as well as its suitability for upscaling to the kW -range scale. Enhancement of the performance directly proportional to the increase of area by design was also demonstrated at the stack level, which has direct implications on the volumetric and mass power density. To conclude, although beyond the scope of this paper, it is important to mention the observed simplification of the dismantling process of the stack (mainly due to the use of compressive sealants enabled by the enhanced mechanical properties of the corrugated cells), which opens the possibility of complete recycling of the components of the system after the end of life of the device.

4. Conclusion

Reversible SOFC/SOEC stacks based on 3D printed cells were successfully fabricated and characterized for the first time. Complex-shaped electrolyte-supported cells based on 3YSZ were optimized to reduce stack volume and weight by design up to three and four times, respectively. This was mainly achieved by embedding interconnector functionality within the printed cells, which straightforwardly reduces the thickness and weight of the stack while simplifying the assembly process and reducing the consumption of raw materials. In particular, stacks based on single repeating units made of corrugated Ni-YSZ/YSZ/LSM-YSZ electrolyte-supported cells sandwiched in thin flat metallic interconnects were manufactured and electrochemically characterized. Substacks of 3 SRUs and full stacks of 18 SRUs were manufactured and measured at 900 °C. Substacks yielded a maximum power of 27 W (200 mW/cm^2) and a maximum injected current of −20 A at 4.2 V (−450 mA/cm^2) in SOFC and SOEC mode, respectively, while complete stacks were able to reach −13 A at 25 V (equivalent to 330 W of power). Continuous operation tests performed for more than 500 h showed small degradation of the stack in the range of 5 %/kh, which proved the durability of the technology in the mid-term. Overall, this study highlights 3D printing as a highly promising and scalable method for achieving complex geometries impossible to reach by conventional manufacturing, which give rise to substantial improvements with respect to conventional technologies only by design (using the same state-of-the-art materials). In particular, our approach paves the way for a novel paradigm in SOFC/SOEC stacks characterized by enhanced power density and mechanical robustness.

CRediT authorship contribution statement

A.M. Martos: Writing – review & editing, Writing – original draft, Investigation. **S. Márquez:** Writing – review & editing, Writing – original draft, Investigation. **R.S. Pavlov:** Writing – review & editing, Investigation. **W. Zambelli:** Writing – review & editing, Investigation. **S. Anelli:** Writing – review & editing, Investigation. **M. Nuñez:** Writing – review & editing, Investigation. **L. Bernadet:** Writing – review & editing, Investigation. **J.J. Brey:** Writing – review & editing, Funding acquisition. **M. Torrell:** Writing – review & editing, Supervision, Investigation, Conceptualization. **A. Tarancón:** Writing – review & editing, Writing – original draft, Funding acquisition, Conceptualization.

Declaration of competing interest

The authors declare that they have no known competing financial interests or personal relationships that could have appeared to influence the work reported in this paper.

Data availability

Data will be available in an open access repository

Acknowledgements

The authors gratefully acknowledge the funding from the European Union through the HyP3D (Grant Agreement No. 101101274). Views and opinions expressed are however those of the author(s) only and do not necessarily reflect those of the European Union nor granting authority can be held responsible for them and also the support from TED2021-131267B-C31 (SIMPEL) project funded by MICIU/AEI/10.13039/501100011033 and by the European Union NextGenerationEU/PRTR. This work has also been partially funded from "Generalitat de Catalunya" Grant No. 2021 SGR 00750. These activities are also part of the Tecnopropia projects, an Important Project of Common Interest (IPCEI) for hydrogen technology within Component 9 of the Recovery, Transformation and Resilience Plan, which has been financed by the European Union-Next Generation EU, through IDEA. Reference PR-IPCEI 2023-000001.

Appendix A. Supplementary data

Supplementary data to this article can be found online at https://doi.org/10.1016/j.jpowsour.2024.234704.

References

[1] S.J. Davis, et al., Net-zero emissions energy systems, Science 360 (2018), https://doi.org/10.1126/science.aas9793.
[2] A. Hauch, R. Küngas, P. Blennow, A.B. Hansen, J.B. Hansen, B.V. Mathiesen, M. B. Mogensen, Recent advances in solid oxide cell technology for electrolysis, Science 370 (2020), https://doi.org/10.1126/science.aba6118.
[3] M. El-Shafie, Hydrogen production by water electrolysis technologies: a review, Resul. Eng. 20 (2023) 101426, https://doi.org/10.1016/j.rineng.2023.101426.
[4] D.M. Bierschenk, J.R. Wilson, S.A. Barnett, High efficiency electrical energy storage using a methane-oxygen solid oxide cell, Energy Environ. Sci. 4 (2011), https://doi.org/10.1039/c0ee00457j.
[5] J. Mermelstein, O. Posdziech, Development and demonstration of a novel reversible SOFC system for utility and micro grid energy storage, Fuel Cell. 17 (2017), https://doi.org/10.1002/fuce.201600185.
[6] S.H. Jensen, C. Graves, M. Mogensen, C. Wendel, R. Braun, G. Hughes, Z. Gao, S. A. Barnett, Large-scale electricity storage utilizing reversible solid oxide cells combined with underground storage of CO2 and CH4, Energy Environ. Sci. 8 (2015), https://doi.org/10.1039/c5ee01485a.
[7] S. Santhanam, M.P. Heddrich, M. Riedel, K.A. Friedrich, Theoretical and experimental study of Reversible Solid Oxide Cell (r-SOC) systems for energy storage, Energy 141 (2017) 202–214, https://doi.org/10.1016/j.energy.2017.09.081.
[8] K.C. Wincewicz, J.S. Cooper, Taxonomies of SOFC material and manufacturing alternatives, J. Power Sources 140 (2005) 280–296, https://doi.org/10.1016/j.jpowsour.2004.08.032.
[9] M. Liu, M.E. Lynch, K. Blinn, F.M. Alamgir, Y. Choi, Rational SOFC material design: new advances and tools, Mater. Today 14 (2011) 534–546, https://doi.org/10.1016/S1369-7021(11)70279-6.
[10] N.H. Behling, History of solid oxide fuel cells, in: Fuel Cells, Elsevier, 2013, pp. 223–421, https://doi.org/10.1016/b978-0-444-56325-5.00006-5.

[11] J.T.S. Irvine, P. Connor, Solid oxide fuels cells: facts and figures: past, present and future perspectives for SOFC Technologies, in: Green Energy and Technology, Springer Verlag, 2013, https://doi.org/10.1007/978-1-4471-4456-4.
[12] M. Singh, D. Zappa, E. Comini, Solid oxide fuel cell: decade of progress, future perspectives and challenges, Int. J. Hydrogen Energy 46 (2021) 27643–27674, https://doi.org/10.1016/j.ijhydene.2021.06.020.
[13] P. Zhu, Z. Wu, Y. Yang, H. Wang, R. Li, F. Yang, Z. Zhang, The dynamic response of solid oxide fuel cell fueled by syngas during the operating condition variations, Appl. Energy 349 (2023), https://doi.org/10.1016/j.apenergy.2023.121655.
[14] T.H. Lim, J.L. Park, S.B. Lee, S.J. Park, R.H. Song, D.R. Shin, Fabrication and operation of a 1 kW class anode-supported flat tubular SOFC stack, Int. J. Hydrogen Energy 35 (2010), https://doi.org/10.1016/j.ijhydene.2010.06.052.
[15] Y. Lu, L. Schaefer, Numerical study of a flat-tube high power density solid oxide fuel cell: Part II: cell performance and stack optimization, J. Power Sources 153 (2006), https://doi.org/10.1016/j.jpowsour.2005.03.189.
[16] Y. Lu, L. Schaefer, P. Li, Numerical study of a flat-tube high power density solid oxide fuel cell: Part I. Heat/mass transfer and fluid flow, J. Power Sources 140 (2005), https://doi.org/10.1016/j.jpowsour.2004.08.036.
[17] F.J. Gardner, M.J. Day, N.P. Brandon, M.N. Pashley, M. Cassidy, SOFC technology development at Rolls-Royce, J. Power Sources 86 (2000), https://doi.org/10.1016/S0378-7753(99)00428-0.
[18] L. Blum, Multi-kW-SOFC development at Siemens. ECS Proceedings Volumes 1995–1, 1995, https://doi.org/10.1149/199501.0163pv.
[19] A. Chesnaud, F. Delloro, M. Geagea, A.-P. Abellard, J. Ouyang, D. Li, T. Shi, B. Chi, R. Ihringer, M. Cassir, A. Thorel, Corrugated electrode/electrolyte interfaces in SOFC: theoretical and experimental development, ECS Trans. 78 (2017), https://doi.org/10.1149/07801.1851ecst.
[20] Z. Masaud, M. Zubair Khan, A. Hussain, H. Ahmad Ishfaq, R.-H. Song, S.-B. Lee, D. W. Joh, T.-H. Lim, Recent activities of solid oxide fuel cell research in the 3D printing processes, Trans. Korean Hydrogen Energy Soc 32 (2021), https://doi.org/10.7316/khnes.2021.32.1.11.
[21] A. Tarancón, Esposito, 3D Printing for Energy Applications, Wiley-American Ceramic Society, 2021.
[22] K. Hosoi, M. Nakabaru, Status of national project for SOFC development in Japan, ECS Trans. 25 (2009), https://doi.org/10.1149/1.3205503.
[23] S.C. Singhal, Solid oxide fuel cells for stationary, mobile, and military applications, in: Solid State Ion, 2002, https://doi.org/10.1016/S0167-2738(02)00349-1.
[24] W. Huang, C. Finnerty, R. Sharp, K. Wang, B. Balili, High-performance 3D printed microtubular solid oxide fuel cells, Adv. Mater. Technol. 2 (2017), https://doi.org/10.1002/admt.201600258.
[25] A. Pesce, A. Hornés, M. Núñez, A. Morata, M. Torrell, A. Tarancón, 3D printing the next generation of enhanced solid oxide fuel and electrolysis cells, J. Mater. Chem. A Mater. 8 (2020) 16926–16932, https://doi.org/10.1039/d0ta02803g.
[26] S. Masciandaro, M. Torrell, P. Leone, A. Tarancón, Three-dimensional printed yttria-stabilized zirconia self-supported electrolytes for solid oxide fuel cell applications, J. Eur. Ceram. Soc. 39 (2019) 9–16, https://doi.org/10.1016/j.jeurceramsoc.2017.11.033.
[27] M. Lira, N. Kostretsova, I. Babeli, L. Bernadet, S. Marquez, A. Morata, M. Torrell, A. Tarancón, Large-area 3D printed electrolyte-supported reversible solid oxide cells, Electrochim. Acta 467 (2023), https://doi.org/10.1016/j.electacta.2023.143074.
[28] M. Lang, C. Auer, A. Eismann, G. Schiller, P. Szabo, Characterization of SOFC Short stacks and stacks for mobile applications, ECS Trans. 7 (2007) 85–94, https://doi.org/10.1149/1.2729077.
[29] K. Jia, L. Zheng, W. Liu, J. Zhang, F. Yu, X. Meng, C. Li, J. Sunarso, N. Yang, A new and simple way to prepare monolithic solid oxide fuel cell stack by stereolithography 3D printing technology using 8 mol% yttria stabilized zirconia photocurable slurry, J. Eur. Ceram. Soc. 42 (2022) 4275–4285, https://doi.org/10.1016/j.jeurceramsoc.2022.03.060.
[30] L. Zheng, R. Xu, J. Zhang, F. Yu, C. Li, J. Sunarso, W. Zhang, X. Meng, N. Yang, Enhanced electrochemical performance by structural design of electrolyte surface combining 3D printing technology with multi-physical modelling, Chem. Eng. J. 451 (2023), https://doi.org/10.1016/j.cej.2022.139038.
[31] H. Huang, Z. Han, S. Lu, W. Kong, J. Wu, X. Wang, The analysis of structure parameters of MOLB type solid oxide fuel cell, Int. J. Hydrogen Energy 45 (2020) 20351–20359, https://doi.org/10.1016/j.ijhydene.2019.10.251.
[32] A. Nakanishi, Development of MOLB type SOFC, ECS Proc. Vol. 2003–07 (2003) 53–59, https://doi.org/10.1149/200307.0053PV.
[33] V.J. Ferreira, D. Wolff, A. Hornés, A. Morata, M. Torrell, A. Tarancón, C. Corchero, 5 kW SOFC stack via 3D printing manufacturing: an evaluation of potential environmental benefits, Appl. Energy 291 (2021) 116803, https://doi.org/10.1016/j.apenergy.2021.116803.
[34] Q. Fang, L. Blum, N.H. Menzler, Performance and degradation of solid oxide electrolysis cells in stack, J. Electrochem. Soc. 162 (2015) F907–F912, https://doi.org/10.1149/2.0941508jes.
[35] S. Pirou, et al., Production of a monolithic fuel cell stack with high power density, Nat. Commun. 13 (2022), https://doi.org/10.1038/s41467-022-28970-w.
[36] W.J. Donahue, O.-H. Kwon, F.M. Mahoney, J.D. Pietras, SOFC Stack Having a High Temperature Bonded Ceramic Interconnect and Method for Making Same, 2007.
[37] J. Carter, R. Kumar, D. Myers, J. Ralph, Metallic bipolar plate-supported solid oxide fuel cell:TuffCell, in: Fuel Cell Seminar, 2004. San Antonio, Texas, USA.
[38] P. Boldrin, N.P. Brandon, Progress and outlook for solid oxide fuel cells for transportation applications, Nat. Catal. 2 (2019) 571–577, https://doi.org/10.1038/s41929-019-0310-y.
[39] R.T. Leah, A. Bone, E. Hammer, A. Selcuk, M. Rahman, A. Clare, L. Rees, N. Lawrence, A. Ballard, T. Domanski, S. Mukerjee, M. Selby, Development of high efficiency steel cell technology for multiple applications, ECS Trans. 78 (2017), https://doi.org/10.1149/07801.2005ecst.
[40] T.L. Cable, S.W. Sofie, A symmetrical, planar SOFC design for NASA's high specific power density requirements, J. Power Sources 174 (2007), https://doi.org/10.1016/j.jpowsour.2007.08.110.
[41] M. Liang, B. Yu, M. Wen, J. Chen, J. Xu, Y. Zhai, Preparation of LSM-YSZ composite powder for anode of solid oxide electrolysis cell and its activation mechanism, J. Power Sources 190 (2009) 341–345, https://doi.org/10.1016/j.jpowsour.2008.12.132.
[42] R. Küngas, Solid Oxide Electrolysis Stack Tests 2010-2019, Figshare, 2020. https://figshare.com/articles/dataset/Solid_oxide_electrolysis_stack_tests_2010-2019/12137112/1. (Accessed 17 January 2024).
[43] J. Schefold, A. Brisse, M. Zahid, J.P. Ouweltjes, J.U. Nielsen, Long term testing of Short stacks with solid oxide cells for water electrolysis, ECS Trans. 35 (2011) 2915–2927, https://doi.org/10.1149/1.3570291.
[44] X. Zhang, J.E. O'Brien, R.C. O'Brien, J.J. Hartvigsen, G. Tao, G.K. Housley, Improved durability of SOEC stacks for high temperature electrolysis, Int. J. Hydrogen Energy 38 (2013) 20–28, https://doi.org/10.1016/j.ijhydene.2012.09.176.
[45] J. Schefold, A. Brisse, M. Zahid, Long term testing of solid oxide fuel cell stacks with yttria stabilized zirconia electrolyte in the H2O electrolysis mode, ECS Trans. 28 (2010) 357, https://doi.org/10.1149/1.3495860.